*Scientia Iranica*, Vol. 7, No. 2, pp 82–91


SCIENTIA
IRANICA

# Approximation of Titration Curves by Artificial Neural Networks and Its Application to pH Control

**M.R. Pishvaie[1] and M. Shahrokhi***

Advanced model-based control of pH processes is noticeably a chemical modeling issue, because it can have a profound effect on the attainable control quality. This is especially the case when the pH regulation of streams, consisting of hundreds of constituents with varying concentrations, is encountered. The severe non-linear behavior of pH processes is reflected in the titration curve of the process stream. The performances of all model-based controllers are highly dependent on the accuracy of the model. Considering a great number of parameters such as dissociation constants, solubility products and characteristic concentrations places the designer in a dilemma of choosing between approximate physicochemical models and empirical ones, both having their own merits and shortcomings. Using radial basis function artificial neural networks, a new modeling approach for approximating the titration curve is proposed in this article and some physical interpretations for selecting the neural network parameters are given. Both off-line and on-line training for adaptive control strategy can be used. The effectiveness of the proposed scheme is demonstrated by simulation and experimental studies.

## INTRODUCTION

The control of pH is not merely a control problem, but also a chemical equilibrium and, sometimes a kinetic problem as well. Advanced control of pH is significantly dependent on the quality of the process model [1]. As demonstrated by several researchers, the highly nonlinear behavior of pH system is reflected in the titration curve of process stream [2-5]. In other words, the most nonlinear term of a system is embedded in static part or algebraic mapping of the state space model in a system theory sense. The dynamic part includes the probable variation of flow rates and process tank level, which have a secondary importance or may be regulated in a separate loop. Consequently, the main focus of this article is based on modeling of titration curves.

There are two fundamentally different philosophies that form the basis of modeling, namely mechanistic (or first principles) and empirical (or ad hoc) modeling. Mechanistic models are derived mainly on the basis of a detailed understanding of underlying mechanisms, or laws, that govern the system behavior. An empirical model, on the other hand, is derived mainly on the basis of specific observed behavior of the system [6]. In this respect, mechanistic models are highly desirable but, generally, difficult to develop. In contrast, empirical models are generally poorer and less informative but easier to develop [7,8]. Having mechanistic modeling in mind, hundreds of characteristic concentrations, solubility products, and dissociation constants are needed to identify the titration curve of a typical waste stream. However, identification and model-based control of a pH process, using empirical models, have been illustrated in much open literature. One class of these methods is based on Artificial Neural Networks-ANN [6,9,10].

In this paper, an attempt has been made to provide a hybrid framework that can support the design of an artificial neural network structure for approximation of the titration curves of streams with unknown compositions.

1. *Department of Chemical Engineering, Sharif University of Technology, Tehran, I.R. Iran.*
* *Corresponding Author, Department of Chemical Engineering, Sharif University of Technology, Tehran, I.R. Iran.*

## PHYSICOCHEMICAL REPRESENTATION OF TITRATION CURVES

Development of physicochemical modeling of titration curves requires understanding of terminology including acid/base definition, electroneutrality constraint, pH and its relation to temperature, to name but a few. In addition, dynamic material balances are also needed when considering the control problem of pH process. In problem formulation, the notation of Wright and Kravaris [2] is used. They have reformulated the pH problem by introducing a reduced state variable and notion of the Strong Acid Equivalent (SAE). In their approach, they have defined the inverse of the titration curve (i.e., its reflection about the 45° line), as given below:

$$T(\mathrm{pH}) = \frac{V_2}{V_1} = -\frac{A(\mathrm{pH}) + \sum_{i=1}^{n} a_i(\mathrm{pH}) x_{1i}}{A(\mathrm{pH}) + \sum_{i=1}^{n} a_i(\mathrm{pH}) x_{2i}}, \qquad (1)$$

where $V_1$ and $V_2$ are initial volume of solution being titrated and volume of titrating solution, respectively. $A(\mathrm{pH})$ is defined as $10^{-\mathrm{pH}} - 10^{\mathrm{pH}-14}$. $x_{1i}$ and $x_{2i}$ are total ion concentrations (of streams) and $a_i(\mathrm{pH})$ is a highly nonlinear function of component dissociation constants and pH.

As stated earlier, Wright and Kravaris introduced a state variable, $X$, to construct a minimal state space realization of the pH process. According to their formulation, the equations describing the system behavior are as follows:

$$V\frac{dX}{dt} = -FX + (1 - X)u, \qquad (2a)$$

$$X(\mathrm{pH}) = \frac{T(\mathrm{pH})}{1 + T(\mathrm{pH})} = - \frac{A(\mathrm{pH}) + \sum_{i=1}^{n} a_i(\mathrm{pH}) C_i}{\alpha - \sum_{i=1}^{n} a_i(\mathrm{pH}) C_i} . \qquad (2b)$$

Equation 2a shows the dynamic behavior of the process and Equation 2b denotes the static or algebraic part. The static part, which is a function of the titration curve of the influent process stream, is the primary concern of this article. It should be also noted that in the above formulation, the following assumptions are made; perfect mixing, constant temperature, ideal solution, monoprotic strong base titrating stream with normality of $\alpha$ and influent stream of well-known $n$ species with corresponding $a_i(\mathrm{pH})$ and concentration $C_i$.

As is clear from Equation 1 or 2b, a nonlinear relation is obtained which is linearly parameterized in terms of $\sum_{i=1}^{n} a_i(\mathrm{pH}) C_i$ or $A(\mathrm{pH})$. In this formulation, solid and complex formations are not considered. When a solid phase is formed, the reaction rate may decrease significantly and, also, the form of the titration curve changes. In addition, one gets break-points and long vertical or nearly vertical parts in $T(\mathrm{pH})$, where pH of the solution is constant or changes very little with addition of base. This is, for instance, the case when $Ca(OH)_2$ is used to neutralize wastewater. Furthermore, if the system contains a metal which can react with the acid or base in the system, the apparent strength of acid changes. It is common that the base anion forms complexes with some, usually heavy, metals. One example is copper which forms complexes with acetates. Practically all anions of organic acids form (stronger or weaker) complexes with metals, the alkali metals being an exception [3].

If the above phenomena are taken into account, the model becomes very complex. When the number of species in the feed stream increases, it also makes the modeling of process very complicated. On the other hand, the empirical models can be developed easier and if sufficient data are collected, the model can provide necessary information required for control purposes. In what follows, modeling of titration curve via ANNs is considered.

## ARTIFICIAL NEURAL NETWORKS REPRESENTATION OF TITRATION CURVES

As mentioned earlier, when the number of species present in the influent process stream increases, Equation 2b becomes very complex. One way to simplify the problem, proposed by Gustafsson and Waller [3], is to replace the multiprotic weak acids with several monoprotic acids. The main idea is to introduce fictitious monoprotic acids. Indeed, they have used the nonlinear physicochemical structure as a basis for modeling and used empirical modeling approach to reduce the parameters of the model. This was done through introduction of fictitious species instead of using several dissociation constants. However, one drawback of this method is the difficulty in specifying the number of fictitious weak monoprotic acids with suitable $pK$ values. In this article, based on the neural network approach, a modeling procedure for approximating the titration curve is proposed. The Radial Basis Function (RBF) neural network is used for modeling of the titration curve (slope) and parameters of the network are selected based on some physical interpretation which will be explained later.

In what follows, first the behavior of RBF neural networks is briefly considered. Next, the similarities of their behavior with the slope of titration curve, namely buffering function, is discussed. Finally, it is shown how the titration curve can be modeled globally using the ANNs.

## RBF Networks

RBFs, also called local receptive fields, with only one hidden layer yield an identification problem that is linear in the parameters. This has a significant impact on the computational efforts needed for finding the optimal values of the parameters [9]. A single-layered neural network using RBFs can approximate any nonlinear function to a desired accuracy [11]. RBF approximation is a traditional technique for interpolation in multidimensional space. For simplicity, in this article, just one-dimensional input space is considered. An RBF expansion with one input and a scalar output generates a mapping $f_r : \Re \rightarrow \Re$ according to:

$$f(x) = w_0 + \sum_{i=1}^{n_c} w_i . g(||x - c_i||), \tag{3}$$

where $x \in \Re, g(\circ)$ is a function from $\Re^+$ to $\Re$, $n_c$ is the number of RBF centers, $w_i, 0 \leq i \leq n_c$ are the weights or parameters, $c_i \in \Re^n, 1 \leq i \leq n_c$ are the RBF centers and $|| \circ ||$ denotes Euclidean norm. The equation can be implemented in a multilayered network (Figure 1), where the first layer is the input, the second layer performs the nonlinear transformation and the top layer carries out the weighted summation only.

Notice that the second layer is equivalent to all hidden layers and the nonlinear operation occurs at the output layer nodes of the neural network with sigmoid functions.

Popular choices for the RBF, $g(||x - c_i||)$, are Gaussian Distribution (GD) function,

$$g(x) = \exp(-||x - c_i||^2/\beta_i^2), \tag{4}$$

Multi-Quadratic function (MQ),

$$g(x) = \sqrt{||x - c_i||^2 + \beta_i^2}, \tag{5}$$

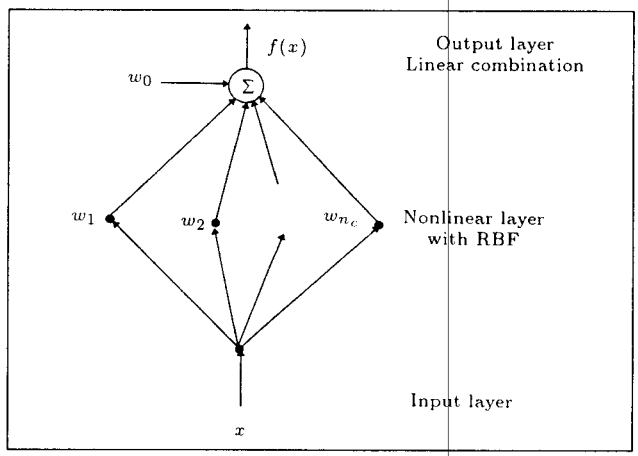


**Figure 1.** One-dimensional neural net structure with RBF.

Reciprocal Multi-Quadratic function (RMQ),

$$g(x) = 1/\sqrt{||x - c_i||^2 + \beta_i^2}, \tag{6}$$

and thin plate spline function,

$$g(x) = ||x - c_i||^2 \log(||x - c_i||), \tag{7}$$

where $\beta_i$ is a scalar width such as standard deviation. The last two functions can provide unbounded output values. However, the first function (i.e., GD function) is considered hereafter. Given the numerical values of the centers $c_i$ and of the width $\beta_i$, determination of the best values of the weights $w_i$ to fit the data is a standard model identification problem which is linear in the parameters. If the centers and/or the width are not predetermined and are adjustable parameters whose values are to be determined along with weights, then the RBF network becomes equivalent to a multilayered feedforward neural network, and an identification which is nonlinear in the parameters must be carried out. Although there are efficient algorithms for choosing the centers and widths (such as k-mean clustering), they are mainly off-line solutions; hence, not suitable for recursive formulation of adaptive control problems.

## Modeling $X'$(pH) Using RBF

Most of the models have a limited range of validity. This means that mechanistic models are valid under certain assumptions and empirical models are applicable for specified ranges. To emphasize this, a model that has a range of validity less than the desired range will be called a local model, as opposed to a global model that will be valid in the full range of operation. As mentioned earlier, the performance of the control scheme is highly dependent on the accuracy of the model. In designing a model based on pH control scheme, knowledge of titration curve plays an important role. On the other hand, it is known that ANN can approximate any complex nonlinear mapping. However, there is no unique structure of ANN for a given problem and the specifications of the network should be determined by trial and error or using nonlinear global optimization techniques like genetic algorithms [12,13]. In the present work, RBFs are used to model $X'$(pH), the derivative of $X$(pH) with respect to pH. By integration of $X'$(pH), the titration curve $X$(pH) is obtained. Theoretical analysis of the validity of such approximation is cumbersome, because general expressions for approximation error cannot be obtained; however, experience indicates that the titration curve for most pH processes can be approximated by this approach.

The typical variations of $X$(pH) and $X'$(pH) vs pH are illustrated in Figure 2. A good candidate for

**Table 1.** Acidic solutions used for simulation studies.

| System | Specifications |
|---|---|
| Example 1 | Monoprotic weak acid with $pK = 6$ and strong monoprotic base as titrating agent with normality 0.03. |
| Example 2 | Mixture of five fictitious monoprotic weak acids with $pK's = [5, 6, 7, 8, 9]$; strong base as titrating agent with normality 0.03. |
| Example 3 | Solution of phosphoric acid ($H_3PO_4$), with concentration of 0.01, titrated by either NaOH or $Ca(OH)_2$. |

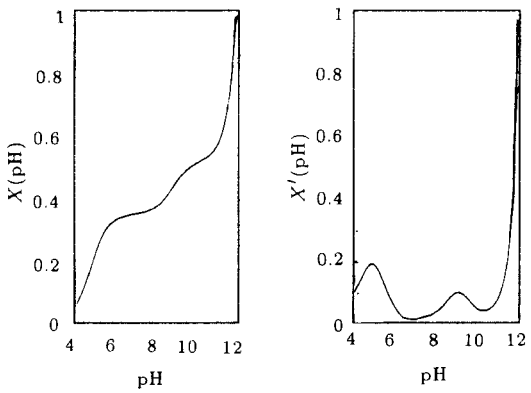


**Figure 2.** A typical titration curve and its derivative.

modeling $X'(\text{pH})$ is an RBF network. As mentioned before, if the numerical values of the centers and widths are known, determination of weights, $w_i$, is a classical linear identification problem. Typical of a titration curve is the jump at the equivalence point. The jump may be very pronounced, as for strong acids and bases, but becomes less pronounced as the strength of acid (or base) diminishes [1]. The vertical jump in a titration curve is reflected in the flattening of $X(\text{pH})$ with respect to pH-axis. The strength of acids (or bases) may also be expressed by the differences in buffering (buffer capacity). Here, buffering or buffer capacity is defined as the inverse of the titration curve slope. The largest buffering at intermediate pH values is obtained at pH = $pK_i$. Buffering quickly decreases when one moves away from pH = $pK_i$, leading to a bell-shaped curvature. Buffering is always high at very low and very high pH values, but in an intermediate and practical range of pH, the species compete with each other by their power of buffering to influence the overall buffering capacity of the system. This phenomena may lead to modeling of the derivative of the titration curve using the weighted sum of the receptive fields of RBF nodes.

To illustrate the procedure of modeling, first a simple case is considered and, thereafter, the technique is extended to more complex systems. Consider a relatively dilute solution consisting of a monoprotic weak acid and a strong base with normality of 0.03. The $pK$ of the weak acid is 6 and its concentration 0.006 M (Example 1). The specifications of systems for other examples, considered later, are given in Table 1.

For modeling $X'(\text{pH})$, Gaussian function $g(x)$ with the following center and width is used:

$$X'(\text{pH}) = w_0 + w_1 \exp\left(-\frac{(\text{pH} - 6)^2}{1}\right). \tag{8}$$

As can be seen from Equation 8, the center is set to the $pK$ value and the width is set to one. Choosing $\beta = 1$ means that the buffering is within the range of one pH unit and setting the center to $pK$ means that the maximum buffering occurs at pH = $pK$. The weights, $w_i$, can be obtained by linear regression and are found for this case as $w_0 = 0.0024$ and $w_1 = 0.0883$. The simulation result is shown in Figure 3. As can be seen, the single node RBF, Equation 8, has approximated the buffering $X'(\text{pH})$ fairly well in the range of pH = 5 to 7.

Another observation is the relation between the sum of the weights, $w_i$, and the peak height. For this example, $w_0 + w_1$ is approximately 0.1, which is equal to the peak height. To check the generality of the above observation, the concentration of the

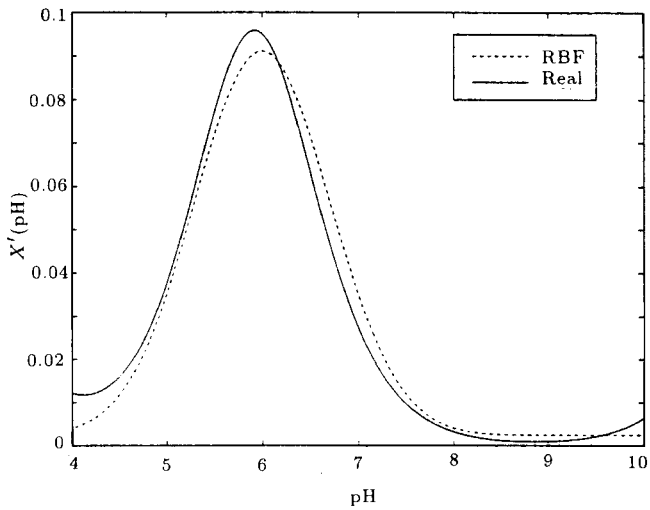


**Figure 3.** Example 1, slope of titration curve with acid concentration of 0.006 M.

acid is increased gradually. Simulation results indicate that as acid becomes more concentrated, the location of the peak center is shifted and moves towards pH $\approx 5.5$.

To compensate for these changes, Equation 8 is modified as follows:

$$X'(\text{pH}) = w_0 + w_1 \exp(-\frac{(\text{pH}-5)^2}{1}) + w_2 \exp(-\frac{(\text{pH}-6)^2}{1}). \quad (9)$$

The simulation for Example 1 was repeated for acid concentration of 0.06 M and using Equation 9, the optimum values of the weights are $w_0 = -0.0131$, $w_1 = 0.2069$ and $w_2 = 0.2216$. Notice that the sum of the weights are nearly equal to the peak height. The actual value of $X'(\text{pH})$ and its estimation are shown in Figure 4. If it is assumed that the maximum buffering occurs at pH = $pK$, Equation 9 can be interpreted as follows. The behavior of the real system is approximated by a solution containing a single multiprotic weak acid with $pK_1 = 5$ and $pK_2 = 6$. This interpretation is in contrast to Gustafsson's assumption of several fictitious monoprotic weak acids [1].

To generalize the above result, the following equation for modeling $X'(\text{pH})$ of any complex solution with the possibility of solid phase or complex formation is proposed:

$$X'(\text{pH}) = w_0 + \sum_{i=1}^{m} w_i \exp(-\frac{(\text{pH}-\text{pH}_{ci})^2}{1}), \quad (10)$$

where $\text{pH}_{ci} = [\text{pH}_{\min}, \text{pH}_{\min}+1, \ldots, \text{pH}_{\max}-1, \text{pH}_{\max}]$, $\text{pH}_{\min}$ and $\text{pH}_{\max}$ are the minimum and maximum pH of the solution. For most practical cases, $\text{pH}_{ci} = [4, 5, 6, 7, 8, 9, 10]$ for which $m$ is 7.

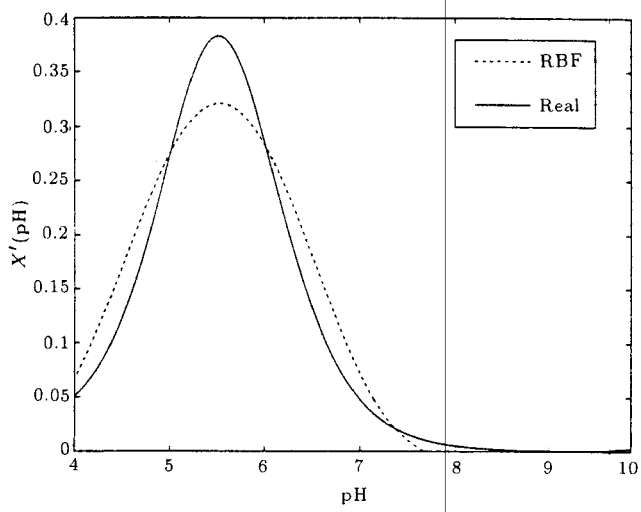


**Figure 4.** Example 1, slope of titration curve with acid concentration of 0.06 M.

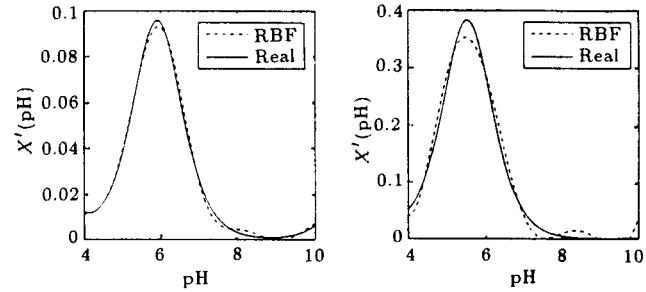


**Figure 5.** Example 1, slopes of titration curves for concentration 0.006 (left) and concentration 0.06 (right) using universal RBF, Equation 10.

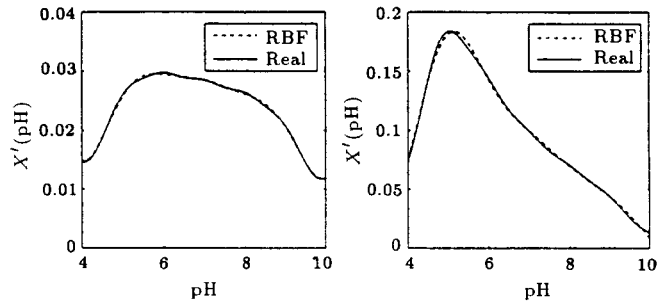


**Figure 6.** Example 2, slopes of titration curves with minimum species concentrations [0.001, 0.001, 0.001, 0.001, 0.001](left) and maximum species concentrations [0.01, 0.01, 0.01, 0.01, 0.01] (right) using universal RBF, Equation 10.

To check the accuracy of the estimation obtained using RBF and given by Equation 10, it is applied to both simple and complex Examples 1 and 2. The data for training the networks are obtained through the simulated pH process. Simulations provide $X(\text{pH})$ and by numerical differentation $X'(\text{pH})$ is obtained. The training sets include the pairs of [pH, $X'(\text{pH})$] starting from pH = 4 and increasing pH by 0.2 pH unit in each interval. Referring to the schematic diagram shown in Figure 1, pH and $X'(\text{pH})$ are network input and output, respectively. The results are shown in Figures 5 and 6. As can be seen, the estimated values of $X'(\text{pH})$ are fairly close to the actual values and the sum of the weights is equal to the peak height. Similar results are obtained if $g(\circ)$ is replaced by RMQ:

$$X'(\text{pH}) = w_0 + \sum_{i=1}^{m} \frac{w_i}{\sqrt{1+(\text{pH}-\text{pH}_{ci})^2}}. \quad (11)$$

## Estimation of Titration Curve Using Integrated RBF

The main objective of this article is to estimate titration curves using neural networks. In the previous section, two equations were developed for estimating

$X'(\mathrm{pH})$ (Equations 10 and 11). By integrating these equations, two expressions for $X(\mathrm{pH})$ can be obtained as follows:

$$X(\mathrm{pH}) - X(\mathrm{pH}^*) = w_0(\mathrm{pH} - \mathrm{pH}^*) + \sum_{i=1}^{m} w_i'\{\mathrm{erf}(\mathrm{pH} - \mathrm{pH}_{ci}) - \mathrm{erf}(\mathrm{pH}^* - \mathrm{pH}_{ci})\}, \quad (12)$$

$$X(\mathrm{pH}) - X(\mathrm{pH}^*) = w_0(\mathrm{pH} - \mathrm{pH}^*) + \sum_{i=1}^{m} w_i\{\sinh^{-1}(\mathrm{pH} - \mathrm{pH}_{ci}) - \sinh^{-1}(\mathrm{pH}^* - \mathrm{pH}_{ci})\}, \quad (13)$$

where $w_i' = (\sqrt{\pi}/2)w_i$ and $\mathrm{pH}^*$ is some reference pH at which the $X(\mathrm{pH}^*)$ is known. Since the model of titration curve is obtained through integration of RBF, it will be called IRBF model (Integrated Radial Basis Function). The advantage of this technique compared to direct modeling of titration curves using the neural network is explained below. If a neural network is used for modeling the titration curve, the structure of the network (parameters of node function, number of nodes,...) should be determined. However, in the proposed scheme, as can be seen from Equations 12 and 13, the structure of the network is determined. This was done by presenting width and centers of RBF nodes through a simple physicochemical justification. Although this structure (i.e., IRBF) is not necessarily the optimum one, it is much simpler than using non-linear programming techniques such as Genetic Algorithms (GAs) or simulated annealing approaches. Furthermore, the proposed scheme is robust to either under-parametrization or over-parametrization problems. The schematic diagram of the proposed network is shown in Figure 7.

Note that the IRBF is principally an empirical model and belongs to the class of ANNs and its power of approximating any complex mathematical mapping should not be neglected. For instance, consider the cases where complex formation or precipitation occurs. Note that if mechanistic modeling approach is used, the constituents present in the feed stream with their dissociation constants should be known.

To demonstrate the effectiveness of IRBF, it is applied to a system where precipitation occurs (Example 3, taken from Gustafsson et al. [1]). The training sets are obtained as described for Examples 1 and 2. The network parameters, $w_i'$, are given in Table 2 and the results are shown in Figures 8 and 9; as can be seen, the titration curves are estimated quite well.

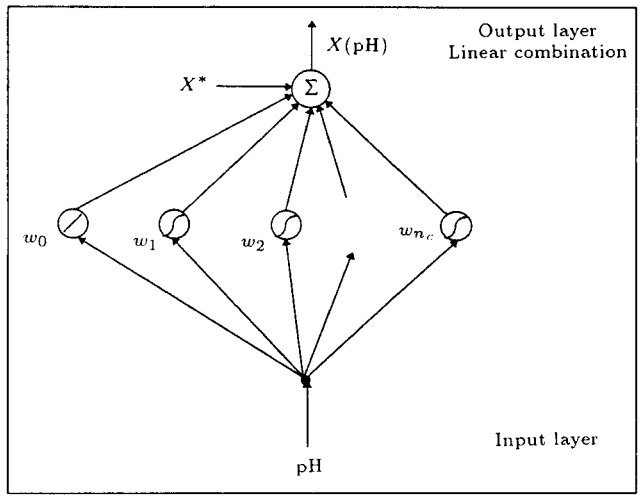


**Figure 7.** Titration curve estimation using universal IRBF.

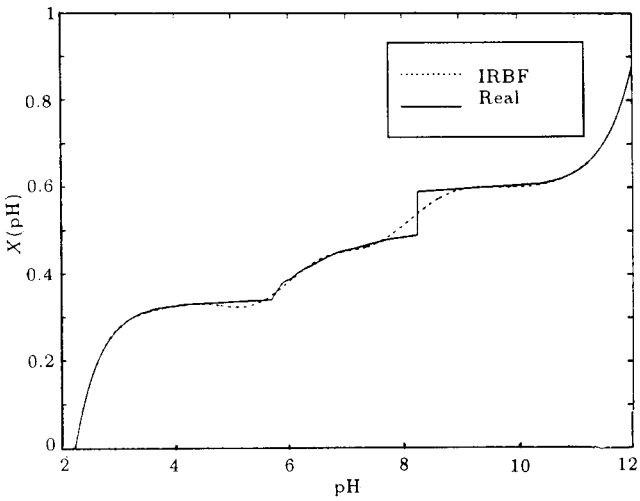


**Figure 8.** Titration curves, Example 3, titrated by calcium hydroxide.

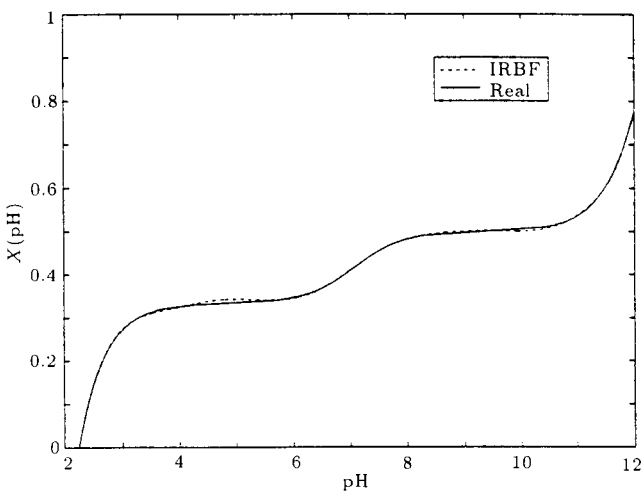


**Figure 9.** Titration curves, Example 3, titrated by sodium hydroxide.

**Table 2.** IRBF network parameters.

| Run | | Parameters | | | | | | | | | | | | |
|---|---|---|---|---|---|---|---|---|---|---|---|---|---|---|
| | | $X^*$ | $w_0$ | $w_1$ | $w_2$ | $w_3$ | $w_4$ | $w_5$ | $w_6$ | $w_7$ | $w_8$ | $w_9$ | $w_{10}$ | $w_{11}$ |
| Example 3 | Using NaOH | 0.410 | 2.351 | -0.905 | -1.387 | -1.278 | -1.342 | -1.334 | -1.230 | -1.327 | -1.314 | -1.351 | -1.265 | -1.308 |
| | Using $Ca(OH)_2$ | 0.453 | 2.199 | -0.791 | -1.321 | -1.160 | -1.346 | -1.056 | -1.337 | -1.099 | -1.252 | -1.253 | -1.196 | -1.192 |
| Open loop experiment | | 0.344 | -0.020 | -0.084 | 0.071 | 0.049 | -0.010 | 0.028 | -0.008 | 0.055 | — | — | — | — |
| Closed loop experiment | Decreasing load | 0.149 | 0.158 | 0.010 | -0.030 | -0.093 | -0.082 | -0.089 | -0.081 | -0.126 | — | — | — | — |
| | Increasing load | 0.355 | 0.154 | 0.007 | -0.079 | -0.079 | -0.083 | -0.098 | -0.044 | -0.122 | — | — | — | — |

## Estimation of Titration Curve Using IRBF and Input/Output Data

As mentioned earlier, most advanced control strategies require knowledge of titration curve. On the other hand, if the influential condition is changed, the titration curve will be affected. Therefore, on-line estimation of titration curve is required. In what follows, based on the expression developed for $X(\mathrm{pH})$, an on-line estimation of titration curve is developed.

For digital control of the system, a discrete model of the process is needed. Assuming that the input is constant between two sample times, the discrete form of Equation 2a becomes:

$$X_k = \gamma_{k-1} X_{k-1} + (1 - \frac{\tau'_{k-1}}{\tau})(1 - \gamma_{k-1}), \tag{14}$$

where $\tau'_{k-1} = \frac{V}{F+u_{k-1}}$, $\tau' = \frac{V}{F}$, $\gamma_{k-1} = \exp(-\frac{T}{\tau'_{k-1}})$ and $X_k = X(\mathrm{pH}_k)$.

If Equation 12 is written for sample times $k-1$ and $k$, it is obtained that:

$$X_k = X^* + w_{0,k-1}(\mathrm{pH}_k - \mathrm{pH}^*) + \sum_{i=1}^{m} w'_{i,k-1}\{\mathrm{erf}(\mathrm{pH}_k - \mathrm{pH}_{ci}) - \mathrm{erf}(\mathrm{pH}^* - \mathrm{pH}_{ci})\}, \tag{15}$$

$$X_{k-1} = X^* + w_{0,k-1}(\mathrm{pH}_{k-1} - \mathrm{pH}^*) + \sum_{i=1}^{m} w'_{i,k-1}\{\mathrm{erf}(\mathrm{pH}_{k-1} - \mathrm{pH}_{ci}) - \mathrm{erf}(\mathrm{pH}^* - \mathrm{pH}_{ci})\}. \tag{16}$$

If $X_{k-1}$ and $X_k$ from the above equations are substituted into Equation 14, it yields:

$$\eta_k = \phi_k^T \Theta, \tag{17}$$

where $\eta_k \triangleq (1 - \frac{\tau'_{k-1}}{\tau})(1 - \gamma_{k-1}), \Theta^T \triangleq [X^*, w_0, w_1, ..., w_m]$ and:

$$\phi_k \triangleq \begin{bmatrix} 1-\gamma_{k-1} \\ \mathrm{pH}_k - \gamma_{k-1}\mathrm{pH}_{k-1} - (1-\gamma_{k-1})\mathrm{pH}^* \\ (\sqrt{\pi}/2)\{\mathrm{erf}_{k,1} - \gamma_{k-1}\mathrm{erf}_{k-1,1} - (1-\gamma_{k-1})\mathrm{erf}(\mathrm{pH}^* - \mathrm{pH}_{c1})\} \\ \vdots \\ (\sqrt{\pi}/2)\{\mathrm{erf}_{k,m} - \gamma_{k-1}\mathrm{erf}_{k-1,m} - (1-\gamma_{k-1})\mathrm{erf}(\mathrm{pH}^* - \mathrm{pH}_{cm})\} \end{bmatrix}$$

$\mathrm{erf}_{k,i} \triangleq \mathrm{erf}(\mathrm{pH}_k - \mathrm{pH}_{ci})$.

The identification error can be defined as:

$$e_k = \eta_k - \Phi_k^T \hat{\Theta}_{k-1}, \tag{18}$$

where $\hat{\Theta}_k$ is the estimated value of $\Theta$. Now, any well-known identification technique such as gradient or least squares can be used for estimating the model parameter $\Theta$. Furthermore, both open loop and closed loop system identification techniques can be used.

### *Experimental Evaluation*

To evaluate the performance of the proposed schemes, a bench-scale pH set-up is used. The schematic diagram of the system is shown in Figure 10. The process consists of acid and base streams, both being fed into the neutralization process tank. The effluent pH is measured as a variable. The base flow rate is regulated by a motorized control valve, while the acid stream is

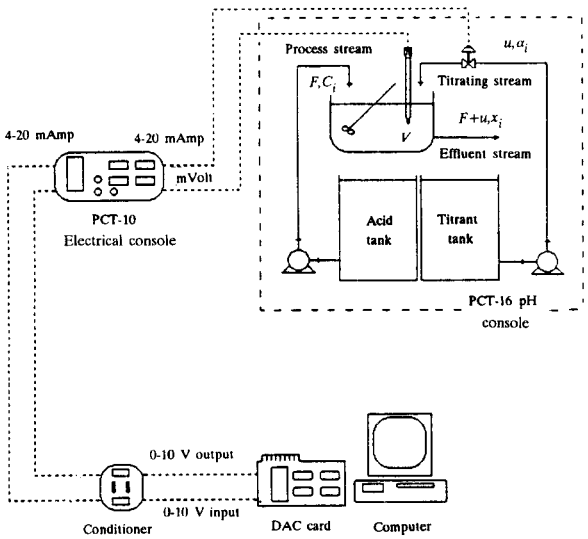


**Figure 10.** Schematic diagram of the experimental system.

**Table 3.** Paramet er values used in the experimental studies.

| | |
|---|---|
| $F = 185$ ml/min | $V = 1720$ ml |
| $u_{ss} \approx 50$ ml/min | $T = 0.1$ min |
| $u_{\min} = 0$ ml/min | $\alpha = 0.03$ N |
| $u_{\max} = 145$ ml/min | $pK_a = 4.78$ |

controlled manually. The level of liquid in the process tank is kept constant by an overflow. The process is monitored and controlled by an IBM compatible PC through an interface card. The main unmeasured load considered for this study is the variation of feed composition.

The feed stream is a diluted acetic acid and caustic soda is used as the titrating agent. The disturbances are produced by injection of pure acetic acid into the process stream reservoir to increase the feed concentration and injection of water to decrease the feed concentration. The parameters of the experimental system are summarized in Table 3. Two sets of experimental runs are performed which are discussed in what follows.

### *Open Loop Identification*

In the open loop experiment, the titration curve is estimated using input-output data obtained through an open loop response. To excite the system, two successive step changes were introduced into the system, as shown in Figure 11. The network parameters are given in Table 2. As can be seen from the result, the network has provided a good estimate of the titration curve for the range of pH variations (train set). The titration curve estimation for the pH values out of the train

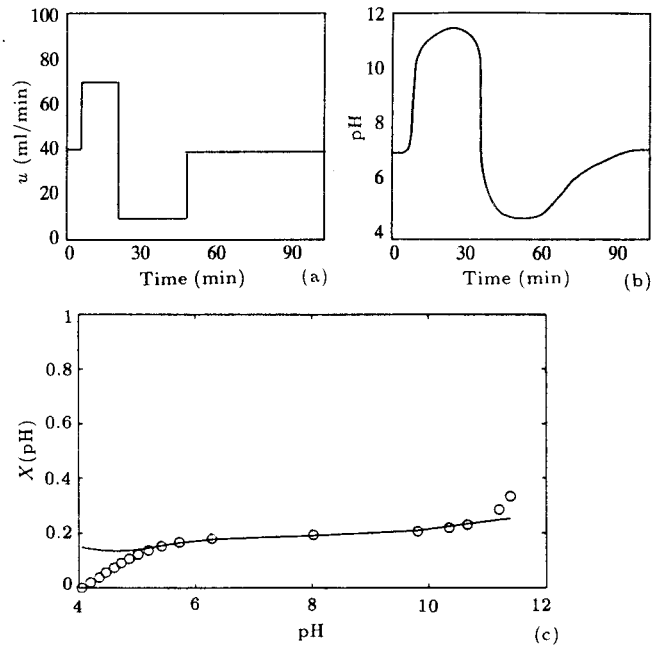


**Figure 11.** Experimental open loop estimation of titration curve, (a) input change, (b) pH variation and (c) real titration curve (bullets) and its IRBF estimation (solid line).

set, however, is not satisfactory. This was expected due to the poor extrapolation capability of empirical models.

### *Closed Loop Identification*

For implementation of adaptive control scheme, on-line estimation of the titration curve is required. To identify the titration curve, the system should be excited which can be done in two different ways; through altering either the set point or the system load. Sung and Lee [14] used the first approach and excited the system through changing the set point. The drawback of this approach is disturbing the system with undesired changes. In the second approach, the titration curve is updated as the system load is changed. In the proposed closed loop identification of titration curve, the second approach is used. Equations 17 and 18 along with recursive least squares method are used for identification. To generate the closed loop data, the non-adaptive strong acid equivalent [2] controller is implemented.

In the first run, the acid concentration is decreased from nominal concentration $8.75 \times 10^{-4}$ M to $1.09 \times 10^{-4}$ M and in the second run it is increased from nominal concentration to $2.19 \times 10^{-3}$ M. The experimental closed loop responses and corresponding titration curve estimates are shown in Figures 12 and 13, respectively. The network parameters are given in Table 2 and the training errors are shown in Figures 14 and 15. The least squares method with a gain of 20I has been selected for on-line training (identification) of

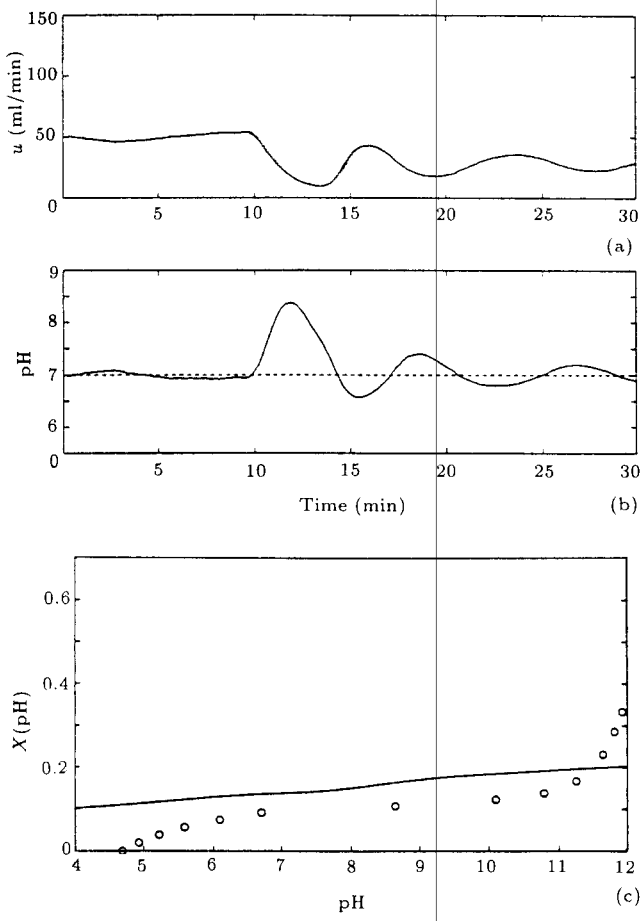


**Figure 12.** Estimation of the titration curve using input/output data for decreasing acid concentration, (a) input change, (b) pH variation and (c) IRBF estimation (bold line) versus experimental titration result (bullets).

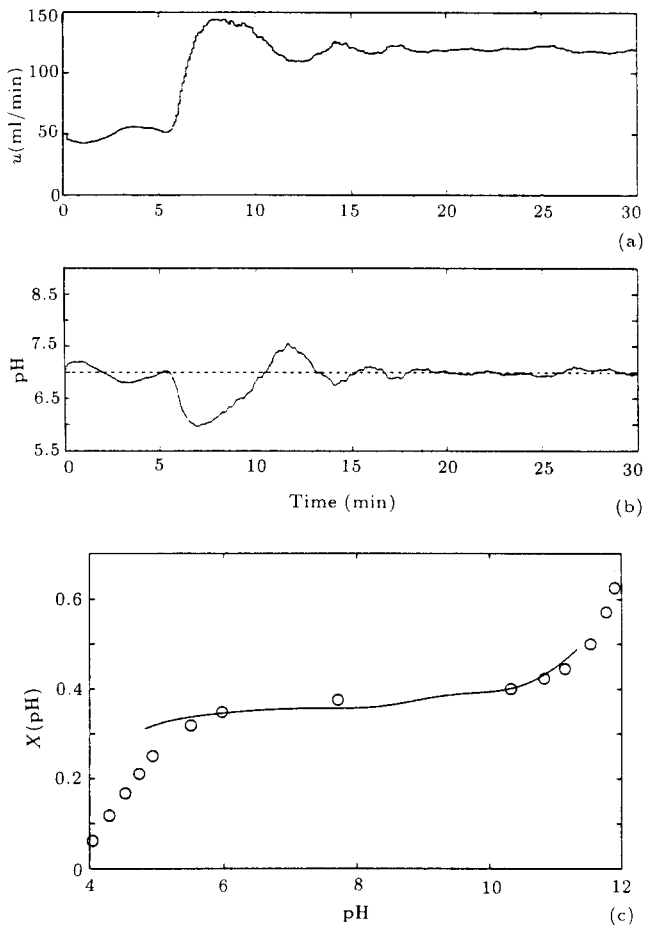


**Figure 13.** Estimation of titration curve, using input/output data for increasing acid concentration, (a) input change, (b) pH variation and (c) IRBF estimations (bold line) versus experimental titration result (bullets).

IRBF. Faster error rate of convergence can be obtained by increasing the initial norm of covariance matrix, but this is limited due to presence of measurement noise.

As can be seen from the results, the IRBF network has estimated the titration curves quite well for the range of pH changes (train set).

## CONCLUSIONS

pH control is a challenging problem due to its highly nonlinear nature. The performance of most control schemes proposed in the literature degrades as the titration curve undergoes large alterations. To overcome this problem, the titration curve should be identified. In this article, the slope of the titration curve is estimated by using an RBF neural network. The values of the centers and width of RBFs are selected by intuition and some physical interpretation. Through integrating the slope of titration curve, an expression is obtained for it. The advantage of the proposed scheme compared to direct modeling

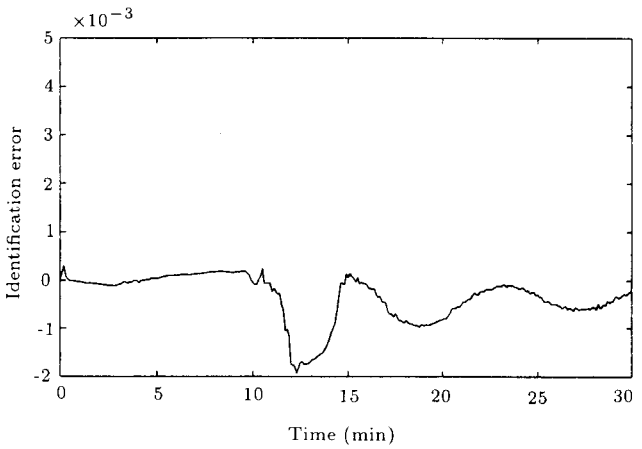


**Figure 14.** Identification error for experimental closed loop (decreasing load) estimation of titration curve.

of titration curve using neural networks is discussed. The off-line estimation procedure is extended to on-line estimation which is very suitable for adaptive control applications. The effectiveness of the proposed

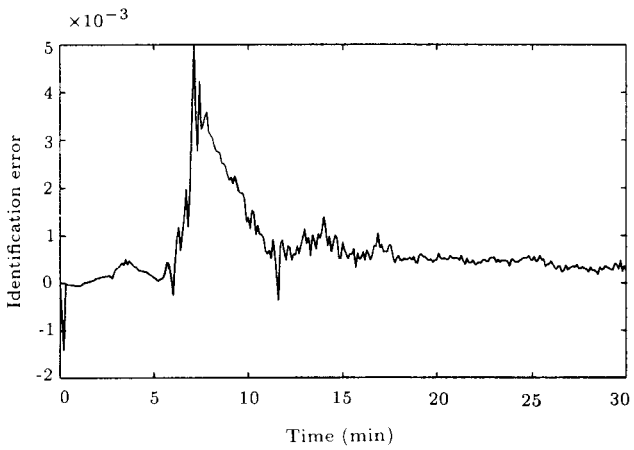


**Figure 15.** Identification error for experimental closed loop (increasing load) estimation of titration curve.

schemes are shown by computer simulations and experiments.

## NOMENCLATURE

| | |
|---|---|
| $A$ | anion of acid |
| $A$(pH) | term depending on pH in general titration curve |
| $a_i$(pH) | pH factor, function of pH that appears as a coefficient of the $i$th ionic total concentration |
| $C_i$ | total ion concentration of the $i$th species in process stream, gmol/l |
| $c_i$ | center of node function |
| erf | error function |
| $F$ | flow rate of process stream, ml/min |
| $g$ | general notation for node function |
| $I$ | identity matrix |
| $K_{ai}$ | $i$th dissociation constant of acid |
| $n$ | number of species |
| $T$ | sampling period of controller |
| $T$(pH) | inverse of standard titration curve |
| $u$ | manipulated variable, flow rate of titrating stream, ml/min |
| $V$ | volume of CSTR, ml |
| $w$ | weight of an ANN node |
| $x$ | general notation of independent variable, input to an ANN |
| $x_i$ | total ion concentration of the $i$th species in effluent stream, gmol/l |
| $X$ | reduced state of system |
| $X'$ | derivative of $X$ with respect to pH |

### Greek Symbols

| | |
|---|---|
| $\alpha_i$ | total ion concentration of the $i$th species in titrating stream, gmol/l |
| $\beta$ | width of Gaussian curve |
| $\tau$ | time constant, min |

## REFERENCES


1. Gustafsson, T.K. et al. "Modeling of pH control", *Ind. Eng. Chem. Res.*, **34**, pp 820-827 (1995).
2. Wright, R.A. and Kravaris, C. "Non-linear control of pH processes using the strong acid equivalent", *Ind. Eng. Chem. Res.*, **30**, pp 1561-1572 (1991).
3. Gustafsson, T.K. and Waller, K.V. "Myths about pH and pH control", *AIChE J.*, **32**, pp 335-337 (1986).
4. Gulaian, M. and Lane, J. "Titration curve estimation for adaptive pH control", *Proc. American Control Conference*, San Diego, CA, USA, p 1414 (1990).
5. Gustafsson, T.K. and Waller, K.V. "Non-linear and adaptive control of pH", *Ind. Eng. Chem. Res.*, **31**, pp 2681-2693 (1992).
6. Johansen, T.A. and Foss, B.A. "Operating regime based process modeling and identification", *Computers and Chem. Engng.*, **21**(2), pp 159-176 (1997).
7. Pearson, R.K. and Ogunnaike, B.A. "Non-linear process identification", in *Nonlinear Process Control*, Chapter 2, Henson, M.A. and Seborg, D.E., Eds., Englewood Cliffs, NJ, USA, Prentice-Hall, pp 11-110 (1997).
8. Marino, R. and Tomei, P. "Global adaptive output-feedback control of non-linear systems: Part II: Non-linear parameterization", *IEEE Trans. Automat Control*, **AC-38**, pp 33-48 (1993).
9. Chen, S. et al. "Recursive hybrid algorithm for non-linear system identification using radial basis function networks", *Int. J. Control*, **55**, pp 1051-1070 (1992).
10. Bhat, N. and McAvoy, T.J. "Use of neural nets for dynamic modeling and control of chemical process systems", *Computers Chem. Engng*, **14**(4/5), pp 573-583 (1990).
11. Cybenko, G. "Approximations by superposition's of a sigmoidal function", *Math. Cont. Signal & Systems*, **2**, pp 303-314 (1989).
12. Goldberg, D. "Genetic algorithms in search, optimization, and machine learning", Addison-Wesley (1988).
13. Whitley, D. "Applying genetic algorithms to neural network learning", Technical Report CS-88-128, Dept. Computer Sci., Colorado State University, USA (1988).
14. Sung, S.W. and Lee, I.B. "pH control using a simple set point change", *Ind. Eng. Chem. Res.*, **34**, pp 1730-1734 (1995).